Aero-Thermal Performance of a Two-Dimensional Highly Loaded Transonic Turbine Nozzle Guide Vane: A Test Case for Inviscid and Viscous Flow Computations

T. Arts

M. Lambert de Rouvroit

von Karman Institute for Fluid Dynamics,
B-1640 Rhode Saint Genèse, Belgium

This contribution deals with an experimental aero-thermal investigation around a highly loaded transonic turbine nozzle guide vane mounted in a linear cascade arrangement. The measurements were performed in the von Karman Institute short duration Isentropic Light Piston Compression Tube facility allowing a correct simulation of Mach and Reynolds numbers as well as of the gas to wall temperature ratio compared to the values currently observed in modern aero engines. The experimental program consisted of flow periodicity checks by means of wall static pressure measurements and Schlieren flow visualizations, blade velocity distribution measurements by means of static pressure tappings, blade convective heat transfer measurements by means of platinum thin films, downstream loss coefficient and exit flow angle determinations by using a new fast traversing mechanism, and free-stream turbulence intensity and spectrum measurements. These different measurements were performed for several combinations of the free-stream flow parameters looking at the relative effects on the aerodynamic blade performance and blade convective heat transfer of Mach number, Reynolds number, and free-stream turbulence intensity.

Introduction

The description of the present test case is a follow-up of similar events, which were presented at the occasion of Lecture Series held at the von Karman Institute for Fluid Dynamics in May, 1973, on "Transonic Flow in Turbomachinery" (Sieverding, 1973) and in April, 1982, on "Numerical Methods for Flows in Turbomachinery Bladings" (Sieverding, 1982). At these occasions, several two and three-dimensional cascade configurations were designed and their aerodynamic performances were experimentally determined as completely and accurately as possible. These measurements mostly served for comparisons with results obtained from inviscid flow calculation methods and presented by different Lecture Series participants. Ever since many other researchers have used the VKI subsonic and transonic turbine cascade test cases to evaluate the accuracy of their two and three-dimensional Euler codes.

A general view on "Test Cases for Computation of Internal Flows in Aero-Engine Components" by AGARD Working Group 18, headed by Prof. Fottner, led to the conclusions that further cascade test cases should provide more information on boundary layer characteristics including heat transfer and turbulence data (Fottner, 1989) for comparison with the numerous Navier–Stokes numerical codes developed over the last years.

Based on these recommendations, the guidelines for the present experiment were established as follows:

- The experimental data should be as reliable as possible and lend themselves to as little criticism as possible. The choice was therefore limited to axial turbine bladings.
- The experimental data should be used for validation of both inviscid and viscous calculation methods. They should provide information on blade velocity distributions, blade convective heat transfer distributions, and downstream loss and flow angle evolutions.

The present experimental program consists of flow periodicity checks by means of wall static pressure measurements and Schlieren flow visualizations, blade velocity distribution measurements by means of static pressure tappings, blade convective heat transfer measurements by means of platinum thin films, downstream loss coefficient and exit flow angle determinations by using a new fast traversing mechanism, and free-stream turbulence intensity and spectrum measurements. These different measurements have been performed for different combinations of the free-stream flow parameters looking at the relative effects of Mach number, Reynolds number, and

Contributed by the International Gas Turbine Institute and presented at the 35th International Gas Turbine and Aeroengine Congress and Exposition, Brussels, Belgium, June 11–14, 1990. Manuscript received by the International Gas Turbine Institute January 26, 1990. Paper No. 90-GT-358.

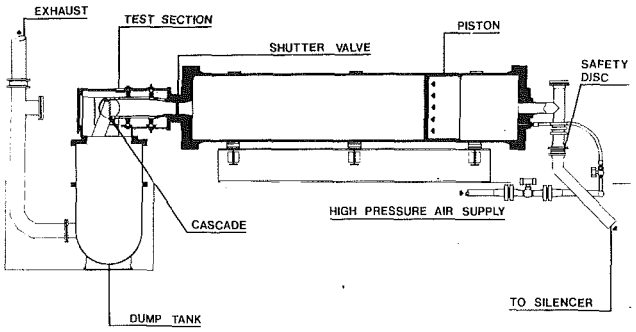

Fig. 1 VKI CT-2 facility

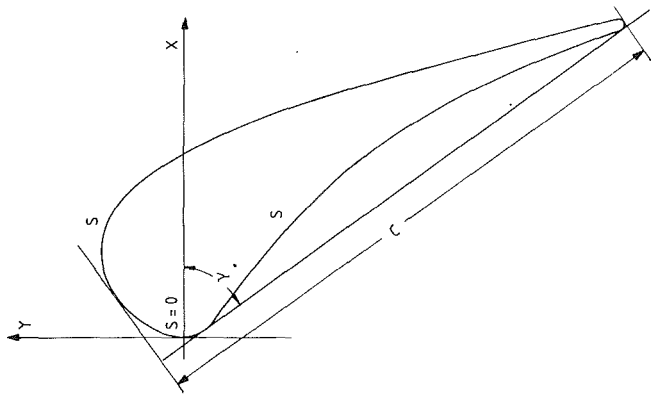

Fig. 2 Geometry of the tested profile

free-stream turbulence intensity on the aerodynamic blade performance and blade convective heat transfer.

A preliminary set of results was presented during the Lecture Series on "Numerical Methods for Flows in Turbomachinery" (Arts et al., 1989) held at the VKI in May 1989, and compared to the numerical predictions provided by a number of participants. The complete, detailed measurement results are available upon request.

Experimental Apparatus

Description of the Facility. The present experimental investigation was carried out in the von Karman Institute Isentropic Light Piston Compression Tube facility CT-2 (Fig. 1). The operating principles of this type of wind tunnel were developed by Jones et al. (1973) and Schultz et al. (1978) about 15 years ago. The VKI CT-2 facility, constructed in 1978, is basically made of three main parts: a 5-m-long and 1-m-dia cylinder, the test section, and a downstream dump tank. The cylinder contains a lightweight piston driven by the air from a high pressure reservoir (...150...250 bar). The cylinder is isolated from the test section by a fast-opening "shutter" or slide valve. As the piston is pushed forward, the gas located in front of it is almost isentropically compressed until it reaches the requested pressure, and hence temperature, levels. The valve is then opened, allowing the pressurized and heated gas to flow through the test section, providing constant free-stream conditions, i. e., total temperature, pressure, and mass flow, until the piston completes its stroke. The free-stream gas total conditions can be varied between 300 and 600 K and 0.5 and 7 bar. The 15-m^3 downstream dump tank allows exit static pressure adjustments between 0.15 and 3 bar. This provides an independent selection of both Mach and Reynolds numbers. The typical test duration is about 400 ms. Air is used as working fluid. Further details about the VKI CT-2 facility have been given by Richards (1980) and Consigny and Richards (1982).

Description of the Model. The different measurements described in the present contribution were carried out on a high-pressure turbine nozzle guide vane profile especially designed for this purpose at the von Karman Institute. The blade shape was optimized for a downstream isentropic Mach number equal to 0.9 by means of an inverse method, developed at VKI by Van den Braembussche et al. (1989). The blade profile is plotted in Fig. 2, whereas its coordinates are listed in Table 1. The blade was mounted in a linear cascade made of five profiles, i.e., four passages. The central blade was instrumented either for static pressure measurements (blade velocity distributions) or for heat flux measurements (blade convective heat transfer distributions). The inlet flow angle to the cascade is 0 deg. The most important geometric characteristics of the cascade are summarized as follows:

c : 67.647 mm
g/c : 0.850
γ : 55.0 deg (from axial direction)
o/g : 0.2597
$r_{LE/c}$: 0.061 (evaluated around stagnation point)
$r_{TE/c}$: 0.0105

Measurement Techniques. Free-stream total pressure and temperature, static pressure, and turbulence intensity were measured 55 mm ($x/c_{ax} = -1.487$) upstream of the leading edge plane, respectively, by means of a Pitot probe, connected to a variable reluctance Valydine differential pressure transducer, a small type K thermocouple probe, wall static pressure tappings connected to National Semi-Conductor differential pressure transducers, and a constant-temperature hot-wire probe. Wall static pressure tappings were also installed downstream of the cascade, in a plane parallel to the trailing edge

Nomenclature

c = chord
d = diameter of bars in turbulence grid
f = frequency
g = pitch
h = heat transfer coefficient
k = isentropic exponent (= 1.4)
M = Mach number
o = throat
p = pressure
$\dot{q}_w$ = wall heat flux
r_{LE} = leading edge radius
r_{TE} = trailing edge radius
Re = Reynolds number
s = coordinate along blade surface
s = pitch of bars in turbulence grid
SPS = pressure side length
SSS = suction side length
T = temperature
Tu = free-stream turbulence
u = velocity
u' = fluctuating component of velocity
V = velocity
x = coordinate along axial chord
y = coordinate in tangential direction
γ = stagger angle
ρ = density

Subscripts

0 = total condition
1 = upstream condition
2 = downstream condition
ax = along the axial chord
is = isentropic condition
w = condition at the wall
∞ = free-stream condition

Table 1 Manufacturing coordinates

SUCTION SIDE					PRESSURE SIDE				
X [mm]	Y [mm]	S [mm]	S/SSS [-]	S/C [-]	X [mm]	Y [mm]	S [mm]	S/SPS [-]	S/C [-]
0.000	0.000	0.000	0.000	0.000	0.000	0.000	0.000	0.000	0.000
0.185	1.554	1.565	0.018	0.023	0.185	-0.913	0.932	0.014	0.014
0.742	3.298	3.401	0.039	0.050	0.927	-2.278	2.512	0.038	0.037
1.484	4.548	4.856	0.056	0.072	1.669	-2.963	3.523	0.054	0.052
2.411	5.859	6.462	0.075	0.096	2.782	-3.852	4.947	0.076	0.073
3.895	7.524	8.695	0.101	0.129	4.081	-4.895	6.613	0.101	0.098
11.871	9.783	17.280	0.200	0.255	9.089	-9.023	13.103	0.201	0.194
18.734	4.705	26.013	0.301	0.385	13.540	-13.062	19.115	0.293	0.283
23.000	-2.663	34.541	0.399	0.511	18.363	-18.038	26.047	0.399	0.385
26.338	-10.988	43.515	0.503	0.643	22.444	-23.229	32.653	0.500	0.483
28.750	-18.713	51.608	0.597	0.763	25.967	-28.850	39.290	0.601	0.581
31.161	-27.615	60.831	0.704	0.899	28.935	-34.724	45.873	0.702	0.678
33.201	-35.897	69.361	0.802	1.025	31.347	-40.456	52.092	0.797	0.770
35.241	-44.337	78.044	0.903	1.154	33.757	-46.920	58.991	0.903	0.872
36.355	-48.941	82.781	0.957	1.224	34.870	-49.950	62.220	0.952	0.920
36.726	-50.476	84.360	0.976	1.247	35.427	-51.465	63.834	0.977	0.944
36.814	-52.087	86.041	0.995	1.272	36.075	-52.312	64.956	0.994	0.960
36.461	-52.305	86.463	1.000	1.278	36.461	-52.305	65.348	1.000	0.966

plane and located 16.0 mm ($x/c_{ax}=1.433$) (measured along the axial chord direction) downstream of the latter. They covered a distance of 130 mm, i.e., a little more than two pitches to verify the downstream periodicity of the flow and to determine the exit Mach number to the cascade. Blade velocity distributions were obtained from 27 static pressure measurements performed along the central blade profile and referred to the upstream total pressure. The downstream loss coefficient evolution as well as the exit flow angle were obtained by means of a fast traversing mechanism, transporting a Pitot probe over two pitches.

Local wall convective heat fluxes were obtained from the corresponding time-dependent surface temperature evolutions, provided by platinum thin-film gages painted onto the central blade, made of machinable glass ceramic. The wall temperature/wall heat flux conversion was obtained from an electrical analogy, simulating a one-dimensional semi-infinite body configuration. A detailed description of this transient measurement technique has been presented by Schultz and Jones (1973). The convective heat transfer coefficient h used in this contribution is defined as the ratio of the measured wall heat flux and the difference between the total free-stream and the local wall temperatures. It is also worth mentioning that the heat transfer measurements discussed in the present paper describe a spanwise averaged behavior as the different thin films were about 20 mm long, but nevertheless situated only in the clean flow region.

Free-Stream Turbulence Generation. One of the important parameters considered in this investigation is the free-stream turbulence. The complete definition of this parameter involves not only its intensity but also its spectrum. These measurements were rather difficult to perform in the CT-2 facility because of the nature of the flow, i.e., an abrupt establishment of a high-speed hot stream, leading to some difficulties in the calibration procedure of the hot-wire probe. The free-stream turbulence was generated by a grid of spanwise oriented parallel bars ($d=3$mm; $s/d=4$). The turbulence intensity was varied by displacing the grid upstream of the model: a maximum of 6 percent could be obtained. The natural turbulence of the facility is about 1 percent. The turbulence intensity quoted in this contribution is defined as:

$$Tu_\infty = \frac{\sqrt{\overline{u'^2}}}{\overline{u}}$$

and was measured using a VKI manufactured constant temperature hot-wire probe. The frequency response of this part

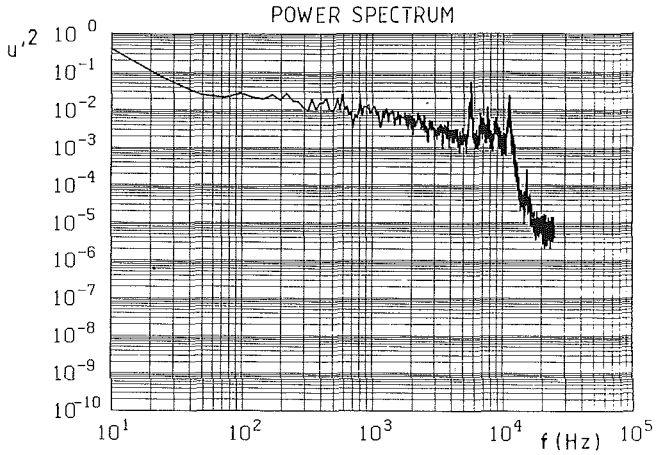

Fig. 3 Free-stream turbulence spectrum analysis

of the measurement chain was observed to be of the order of 10 kHz.

In order to measure the free-stream turbulence spectrum, the raw signal of the hot-wire probe was processed by means of a Fast Fourier analysis. A typical example is shown in Fig. 3. This result is representative of a 4 percent turbulence intensity. Discrete peaks are observed at 5.5 and 11 kHz. In order to investigate the nature of this phenomenon and to determine whether it could have any influence on the boundary layer development, a microphone was mounted inside the test section. The fluctuating component of the output signal was also processed by a Fast Fourier Transform. This analysis revealed the existence of peaks similar to those from the hot-wire signal. Therefore they are obviously of acoustic nature. The information accumulated on this subject up to now seems to indicate that no effect on the boundary layer development is expected from those frequencies. Further investigations on this subject are currently underway at the VKI for high-speed as well as low-speed flows.

Data Acquisition System. All pressure, temperature, and heat flux measurements were directly acquired by a VAX 11/780 computer by means of a VKI manufactured 48 channel data acquisition system through a direct memory access principle. The analog (± 5.0 V) signals were digitized using 12 bit words. For the present measurements, the sampling rate was selected to be 1 kHz for pressure, temperature, and heat flux measurements and 25 or 50 kHz for turbulence intensity and spectrum measurements.

Measurement Uncertainty. The uncertainty on the various measured quantities was carefully evaluated and led to the following error bars, based on a 20:1 confidence interval. The uncertainty on pressure measurements was of the order of ± 0.5 percent, on temperature measurements of the order of ± 1.5 K, on the heat transfer coefficient of the order of $\pm$ 5 percent, on the integrated loss coefficient of the order of $\pm$ 0.2 points, and on the exit flow angle of the order of ± 0.5 deg.

Test Conditions

The test program was built up by varying the free-stream conditions according to the following limits:

T_{01} : 420 K
$M_{2,is}$: 0.70...1.10
$Re_{2,is}$: 0.5 10^5...2.0 10^6
Tu_∞ : 1.0...6.0%

The different flow conditions were defined by all possible combinations of these parameters. All the tests were conducted at least twice to verify the repeatability of the results.

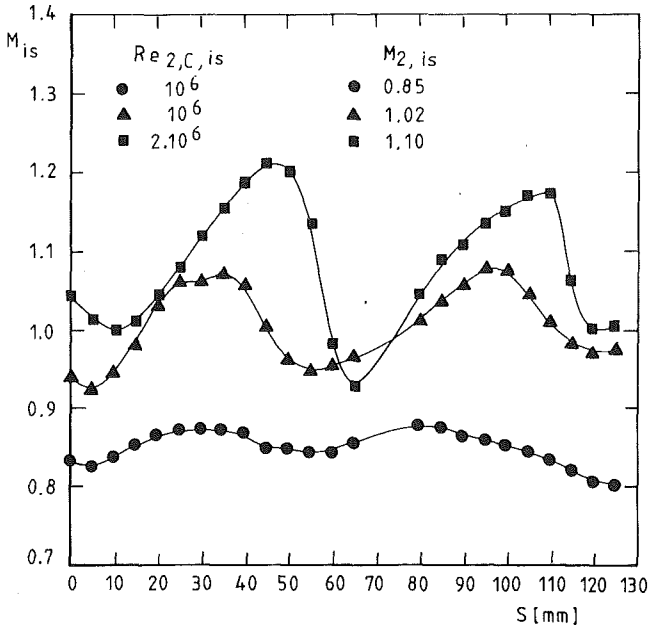

Fig. 4 Downstream static pressure measurements

Periodicity of the Flow

In order to model the flow in a cascade correctly, one must ensure periodic inlet and outlet conditions. The higher the number of blades, the easier it is to establish periodic flow conditions, but for aerodynamic measurements one generally considers eight to ten blades to be a minimum. In the present experiment, however, the scale of the blade has been chosen as large as possible to allow a dense instrumentation, required by the particular goal of this investigation. As a result, only five profiles, i.e., four passages, were used. A careful verification of the flow periodicity was therefore absolutely necessary. Distributions of the downstream wall static pressure were measured and Schlieren flow visualizations were performed for different exit Mach and Reynolds number values. The effect of turbulence intensity was not considered; the measurements were conducted without turbulence grid ($Tu_\infty = 1$ percent).

The downstream static pressure measurements were performed in a plane parallel to the trailing edge plane, located at $x/c_{ax} = 1.433$. The different pressure tappings, located 5 mm from each other, covered 130 mm, i.e., a little more than two pitches. Each tapping was connected to a National Semi-Conductor differential pressure transducer; the low-pressure port of the latter was connected to a vacuum pump to allow a continuous calibration of the system. In order to calculate the downstream flow Mach and Reynolds numbers correctly, the upstream total pressure and temperature were also measured (see section 2.3). The frequency response of the pressure instrumentation was of the order of 150 Hz; the sampling rate was set at 1 kHz. All tests were performed for an upstream total temperature of about 420 K. The useful testing time was of the order of 450 ms. The results are presented as isentropic downstream Mach number distributions versus a coordinate measured along the pitch, toward the lowest profile of the cascade and basically capturing the wakes of blades 3 (the central profile of the cascade) and 4. From these results the averaged exit isentropic Mach number of the cascade was calculated. Based on these measurements, the flow proved to be reasonably periodic for $M_{2,is}$ up to 1.15, as can be seen, e.g., from Fig. 4. Similar measurements were repeated for different downstream Reynolds numbers ranging from 5.0×10^5 to 2.0×10^6; they provided the same conclusions.

Flow visualizations were obtained in the transonic regime

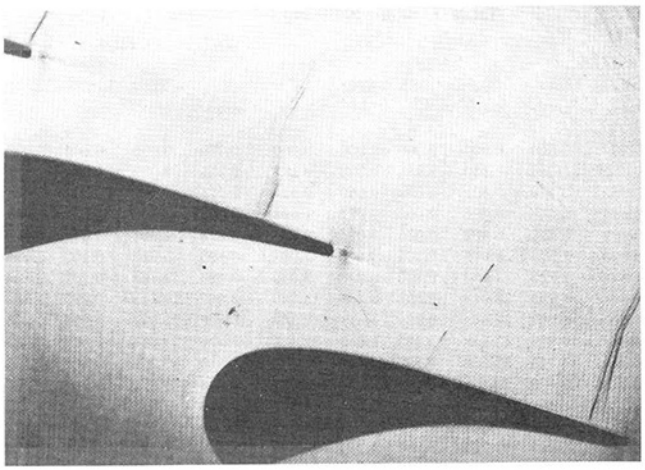

Fig. 5 Schlieren visualization: $M_{2,is} = 1.03$, $Re_{2,is} = 10^6$

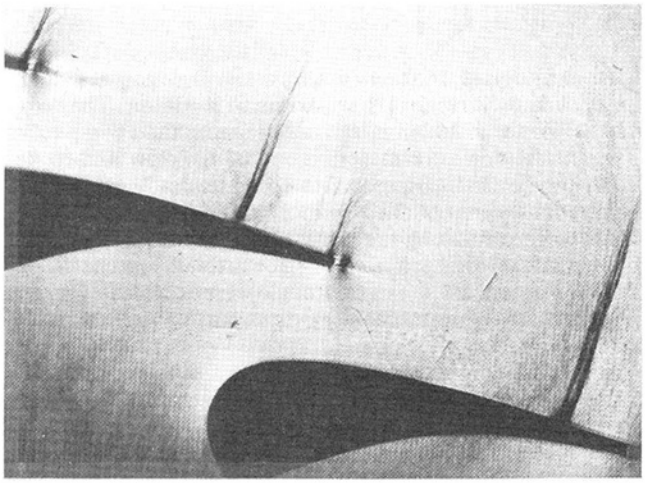

Fig. 6 Schlieren visualization: $M_{2,is} = 1.03$, $Re_{2,is} = 2.0 \times 10^6$

from a single-pass Schlieren system. Figures 5 and 6 present typical results obtained for $M_{2,is} = 1.03$ and $Re_{2,is} = 10^6$ and 2.0×10^6, respectively. Profiles 3 (the central profile of the cascade) and 4 are shown on these pictures. The spark was initiated about 150 ms after the beginning of the test, to be sure that the flow was correctly established in the cascade. A normal shock is observed on the rear part of the suction side; no definite separated flow regions can clearly be identified for any value of the Reynolds number. These visualizations confirm the periodic character of the downstream flow. For values of $M_{2,is}$ in excess of 1.2, however, the flow periodicity deteriorates very quickly. Additional measurements are presently underway to overcome this difficulty by modifying the downstream tailboard arrangement.

Blade Velocity Distributions

Blade isentropic Mach number distributions were obtained for different loadings from local static pressure measurements, referred to the upstream total pressure. The central blade of the cascade was therefore replaced by a similar profile equipped with 27 static pressure tappings, each of then connected to a National Semi-Conductor differential pressure transducer; the low-pressure ports were again connected to a vacuum pump to allow a regular verification of the calibration characteristics. The uncertainty on the measurements, the frequency response of the measurement chain, and the sampling rate have been quoted in sections 2.6 and 4. The repeatability of results was verified and proved to remain within 0.5 percent. The influence of free-stream turbulence intensity and Reynolds number on

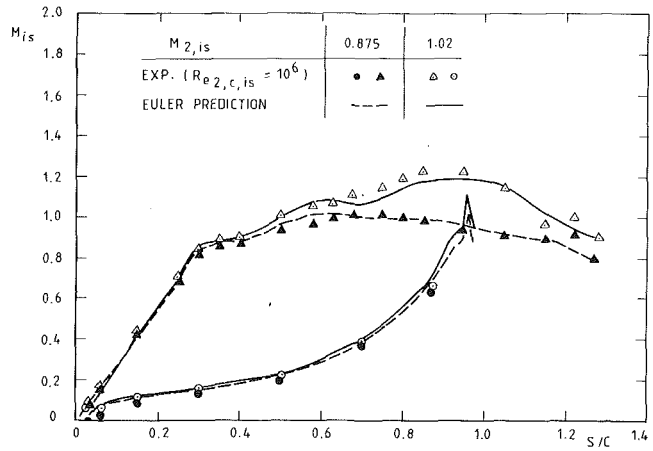

Fig. 7 Blade velocity distributions

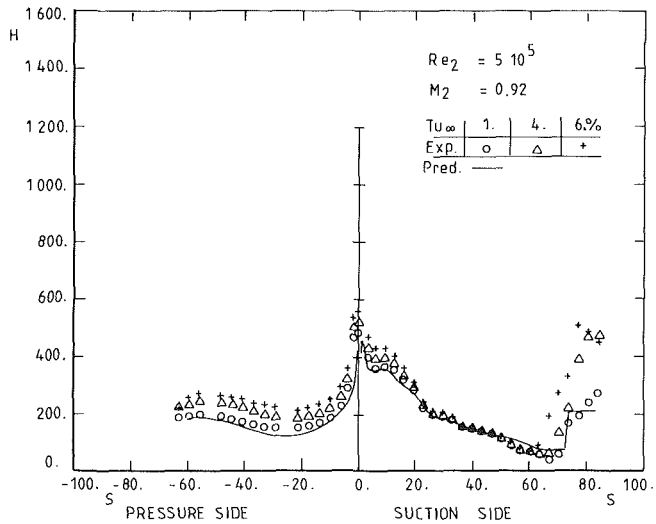

Fig. 8 Blade heat transfer distributions: $M_{2,is} = 0.92$, $Re_{2,is} = 5.0 \times 10^5$

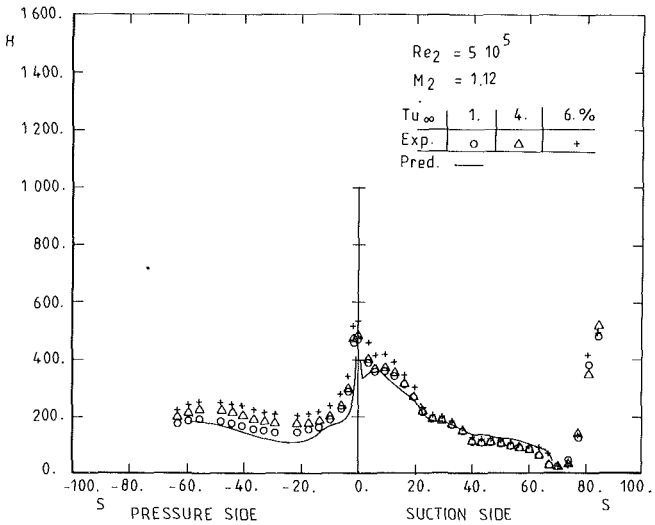

Fig. 9 Blade heat transfer distributions: $M_{2,is} = 1.12$, $Re_{2,is} = 5.0 \times 10^5$

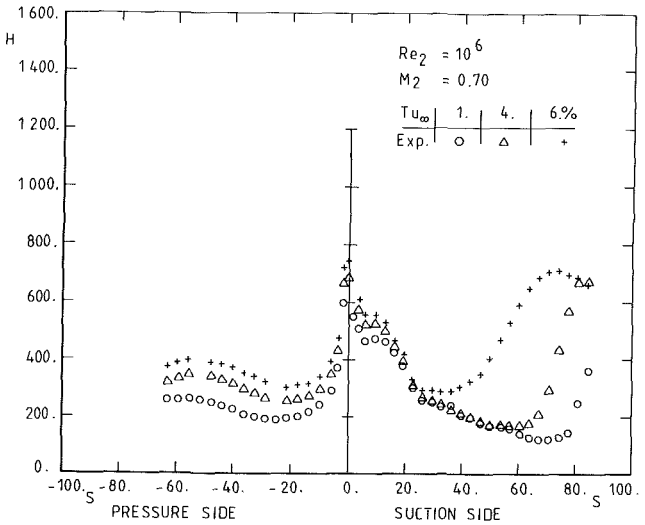

Fig. 10 Blade heat transfer distributions: $M_{2,is} = 0.70$, $Re_{2,is} = 10^6$

the blade velocity distributions were not considered at this stage. All tests were performed for an upstream total temperature of about 420 K. The useful testing time was of the order of 450 ms.

Typical measurement results are presented in Fig. 7. They are plotted as an isentropic Mach number evolution in function of a reduced coordinate (s/c) measured along the profile surface, starting from $x/c_{ax} = 0$. Starting from this theoretical stagnation point, the flow accelerates steeply along the suction side up to $s/c = 0.3$. A small plateau ($s/c = 0.35 \ldots 0.40$) is followed by a reacceleration. For the lowest exit Mach number ($M_{2,is} = 0.875$), the velocity distribution is then rather flat with a weak adverse pressure gradient starting from $s/c \approx 0.75$. Let us remember that the blade was initially designed and optimized for about this value of the exit Mach number. For the higher exit Mach number ($M_{2,is} = 1.02$), the flow accelerates up to $s/c \approx 0.85 \ldots 0.95$. A shock is then observed ($s/c = \ldots 1.05 \ldots$); this position is consistent with the one deduced from the Schlieren pictures. The velocity distribution along the pressure side varies smoothly, with no evidence of a velocity peak downstream of the leading edge.

The measurements were compared to the results obtained from a two-dimensional inviscid prediction code (Arts, 1982), based on a time-marching integration technique and a finite volume discretization method. For a subsonic exit Mach number, the calculated results nearly match the measured data (Fig. 7). For transonic exit Mach numbers, only small differences are observed.

Blade Heat Transfer Distributions

Blade convective heat transfer distributions were obtained for different Mach and Reynolds numbers and free-stream turbulence intensities by means of 45 platinum thin films, painted on a machinable glass ceramic blade replacing the central profile of the cascade. The frequency response of the measurement chain associated with the thin films (gages, analogs, amplifiers) is far above 1 kHz. The sampling rate was selected to be 1 kHz, and the signals were filtered at 800 Hz. The useful testing time was of the order of 300 ms. The repeatability of the results was verified and proven to remain within 1 percent. All tests were performed for an upstream total temperature of about 420 K. The different results are presented on Figs. 8 to 14 under the form of a heat transfer coefficient distribution ($W/m^2/K$; see section 2.3) versus a length (mm) measured along the suction and pressure sides of the blade, starting from the theoretical stagnation point ($x/c_{ax} = 0.$).

Influence of Free-Stream Turbulence. The influence of free-stream turbulence is presented in Figs. 8 to 14 for three different Mach and Reynolds numbers. The turbulence intensity was varied between 1.0 and 6.0 percent. At low Reynolds numbers (Figs. 8 and 9), Tu_∞ mainly affects the laminar part of the boundary layer. After having reached relatively high

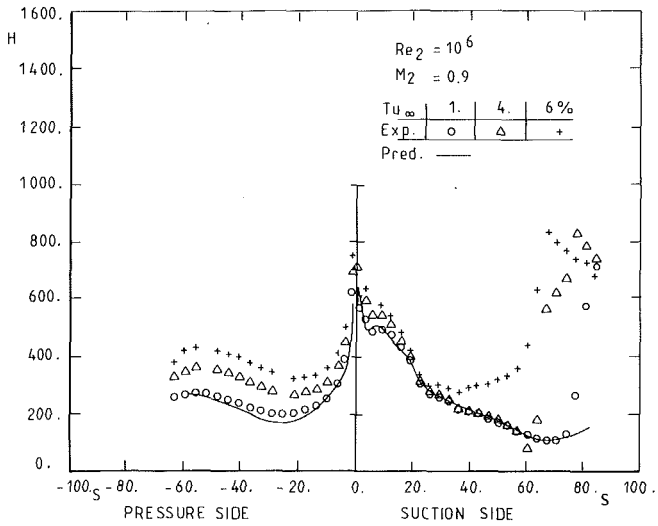

Fig. 11 Blade heat transfer distributions: $M_{2,is} = 0.90$, $Re_{2,is} = 10^6$

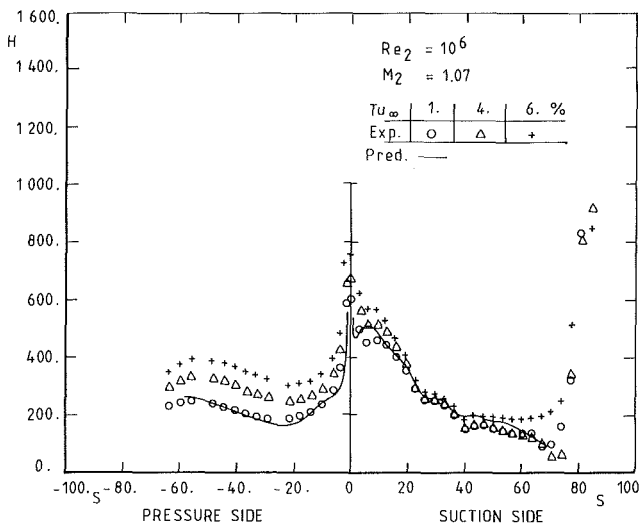

Fig. 12 Blade heat transfer distributions: $M_{2,is} = 1.07$, $Re_{2,is} = 10^6$

values in the region of the leading edge, the heat transfer falls quite rapidly on either side of the blades; this behavior corresponds to the development of a laminar boundary layer. The level of heating is slightly but distinctly increased by increasing Tu_∞; this effect is, however, less important than at the stagnation point. Similar results were obtained for constant pressure and accelerating laminar boundary layers developing on a flat plate (Smith and Kuethe, 1966). For the lowest Mach number ($M_{2,is} = 0.92$) (Fig. 8), the position of the transition onset (s = 62...68 mm) on the suction side does not seem to be greatly affected by Tu_∞. For the highest Mach number ($M_{2,is} = 1.12$) (Fig. 9), the boundary layer transition starts at the shock position ($s = 71.0$ mm). These measurements confirm the shock location observed from the Schlieren pictures and the velocity distributions. Along the pressure side, the boundary layer is most probably in a laminar state.

Similar conclusions are drawn for the intermediate Reynolds number value (Figs. 10, 11, 12), and for the two lowest values of Tu_∞ ($Tu_\infty = 1$ and 4 percent). For the highest value ($Tu_\infty = 6$ percent), however, the onset of transition is observed earlier along the suction side. This position corresponds to the small plateau observed on Fig. 7 along the suction side ($s/c = 0.36$; $s = 24.0$ mm). This phenomenon is not marked for the highest exit Mach number where the acceleration rate is high enough to prevent the onset of transition. The behavior along the

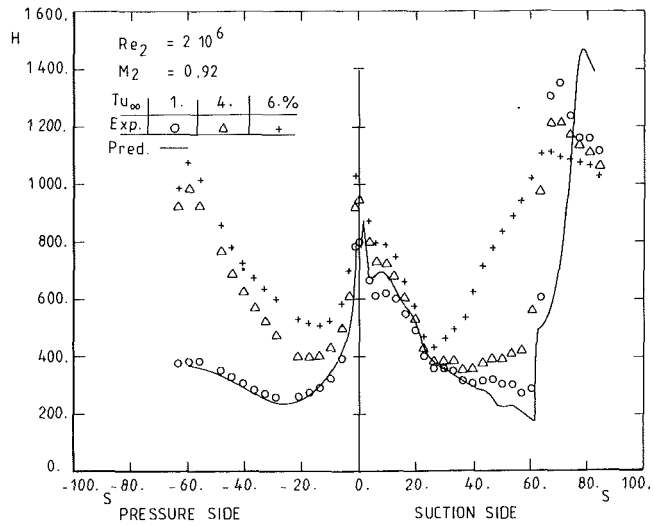

Fig. 13 Blade heat transfer distributions: $M_{2,is} = 0.92$, $Re_{2,is} = 2.0 \times 10^6$

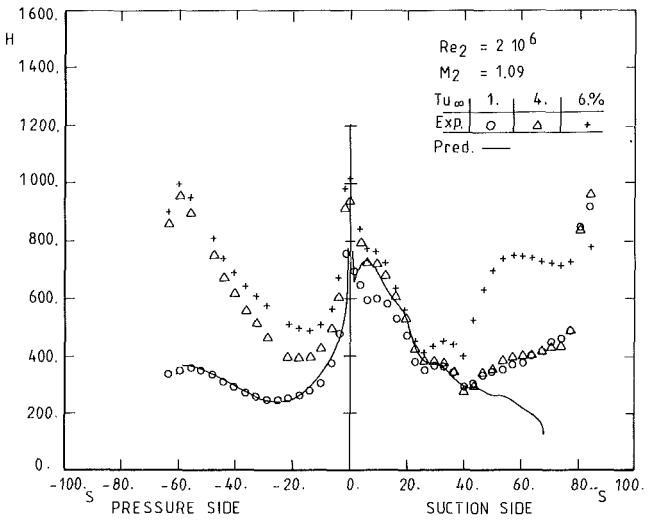

Fig. 14 Blade heat transfer distributions: $M_{2,is} = 1.09$, $Re_{2,is} = 2.0 \times 10^6$

pressure side is rather similar to what has been observed for $Re_{2,is} = 5.0 \times 10^5$

The behavior of the boundary layer seems to be quite different for the highest value of the Reynolds number (Figs. 13 and 14). Along the suction side, it appears that the transition onset is very much influenced by the velocity distribution (Fig. 7). It appears in the present case that this transition is triggered by the first important decrease in velocity gradient. Along the pressure side the boundary layer is much more sensitive to free-stream turbulence. It appears that a fully turbulent state is obtained for the highest value of Tu_∞.

Influence of Free-Stream Reynolds Number. The influence of free-stream Reynolds number is deduced by comparing Figs. 8 to 14. Different Mach numbers and free-stream turbulence intensities were considered. The Reynolds number was varied between 5.0×10^5 and 2.0×10^6. The first effect of Reynolds number is, as expected, to increase the overall level of heat flux. This seems to be the only significative effect at low turbulence intensity ($Tu_\infty = 1$ percent). For $M_{2,is} = 0.92$, the suction side boundary layer transition onset seems to depend only on the velocity distribution, whereas for $M_{2,is} = 1.10$, the start of transition moves toward the leading edge for the highest value of the Reynolds number. The boundary layer is more sensitive to the acceleration changes along this surface. Along the pressure side the boundary layer remains in a laminar/transitional state.

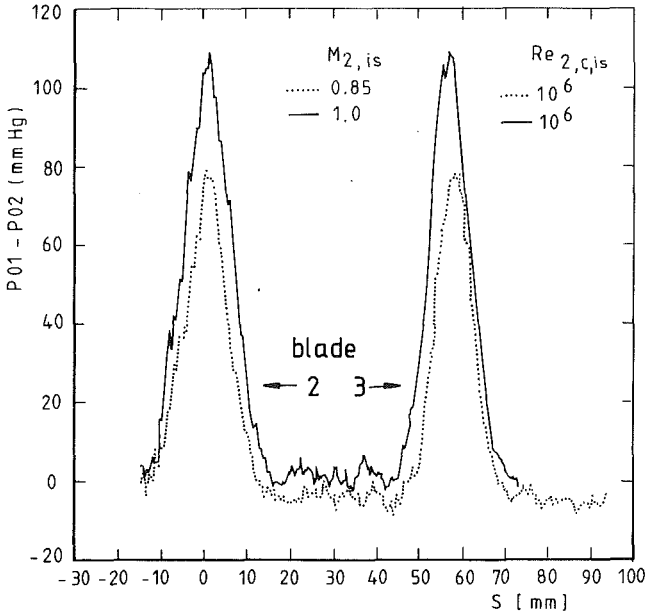

Fig. 15 Measured downstream wakes

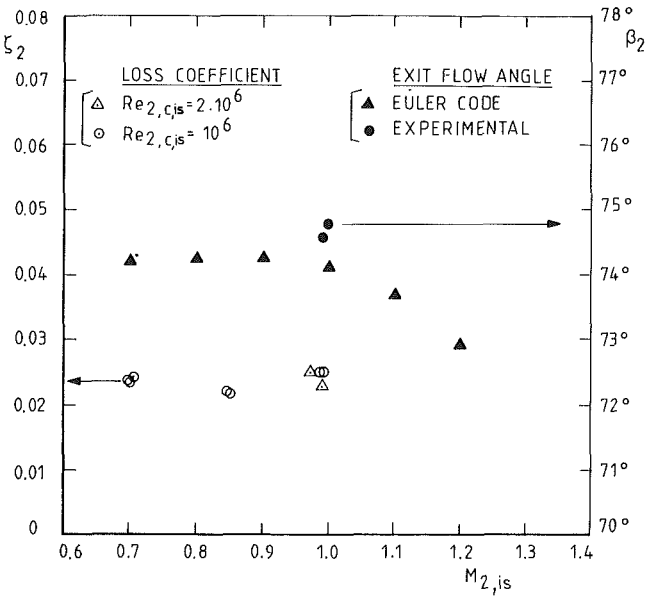

Fig. 16 Downstream loss coefficient and flow angle

For the intermediate turbulence intensity ($Tu_\infty = 4$ percent), similar conclusions can be drawn along the suction side. Along the pressure side, however, the increase in heat transfer is much more important for the highest value of $Re_{2,is}$. For the highest value of turbulence intensity ($Tu_\infty = 6$ percent), the transition of the suction side boundary layer moves gradually upstream with increasing Reynolds number for the two values of the Mach number. For $M_{2,is} = 1.1$ and $Re_{2,is} = 2.0 \times 10^6$, the stabilizing effect of the favorable pressure gradient is clearly observed between $s = 25$ mm (onset of transition) and $s = 40$ mm.

Influence of Free-Stream Mach Number. The influence of free-stream Mach number is deduced by comparing Figs. 8 to 14. Along the pressure side, the velocity distributions are almost similar. As a result, no significative differences appear in the heat transfer coefficient distributions for a given value of the Reynolds number. The behavior of the suction side boundary layer is basically a function of the different acceleration rates observed in Fig. 7.

Numerical Predicitons. An attempt was made to predict these heat transfer measurements numerically. A two-dimensional boundary layer code "TEXSTAN" (Crawford, 1988) was used for this purpose. This program is based on the classical Spalding–Patankar approach (1967) to compute boundary layer or pipe flows. It uses a finite difference technique to solve, through a streamwise space marching procedure, the simplified two-dimensional boundary layer equations as applied to flows developing along, e.g., a flat wall or in an axisymmetric tube. In the present paper, the modeling of the turbulent quantities was provided through a Prandtl mixing length approach. The initial velocity and enthalpy profiles were determined 0.5 mm downstream of the theoretical stagnation point by means of the analytical solution of laminar flow around a cylinder (Schlichting, 1968). The predictions (full line) are compared with the measurements (open symbols) on Figs. 8 to 14. This boundary layer code performs rather well as far as laminar boundary layers are concerned, both on the suction side and on the pressure side. The weak point remains the prediction of the suction side transition onset. Attempts were made to use more sophisticated two-equation turbulence models provided into the program (Crawford, 1985). This led to rather disappointing comparisons. More work should be performed in this area from a transition modeling point of view.

Downstream Loss Coefficient and Angle Distributions

Although the VKI CT-2 facility was originally designed for convective heat transfer measurements only, it is evident that it would also be extremely attractive for aerodynamic performance measurements, if the problems related to the short running time ... 400 ... ms and the relatively high air temperature of 400 ... 450 K could be overcome. The first problem was solved by designing a fast traversing mechanism, transporting a Pitot probe at a maximum speed to 800 mm/s over at least two pitches in a plane parallel to the trailing edge plane. The probe carriage is driven by a pneumatic piston. The traversing speed is controlled by the air supply pressure and choked air bleeds. The position of the probe is measured by a linear variable differential transducer. The frequency response of the complete system was evaluated to be 150 Hz. The second problem was solved by locating the transducer outside of the wind tunnel, taking advantage of the conduction effect in the pneumatic pipe between the head of the probe and the transducer. The probe used with this carriage is a classical total, left/right pressure probe except for the absence of the cone head for the static pressure, which was taken instead from the side wall pressure tappings. The performance and accuracy of the complete system were demonstrated in an earlier paper (Sieverding et al., 1988).

Rigorously constant downstream conditions, imperative for this type of measurement, were ensured downstream of the cascade (even with a closed dump tank) by means of a second sonic throat. The total pressure heads of the upstream and downstream Pitot probes were connected respectively to the high and low-pressure ports of a National Semi-Conductor differential pressure transducer, providing a direct measurement of Δp_{01-02}. The left and right heads of the downstream probe were connected to the two ports of a variable reluctance Valydine differential pressure transducer, providing a measure of Δp_{LR}, proportional to the exit flow angle. The downstream probe was inclined in such a way to have its head located in the same axial plane ($x/c_{ax} = 1.433$) as the wall static pressure tappings already described in section 4. The sampling rate was set at 4 kHz to have a sufficient number of points to resolve the wake. The influence of free-stream turbulence has not been considered up to now. All tests were performed for an upstream total temperature of about 415 K. The useful testing time was of the order of 250 ms.

Typical examples of measured wakes are shown in Fig. 15

($M_{2,is}=0.85$, 1.0). They correspond from left to right to the wakes of blades 2 and 3 (central blade). The resolution of the deepest point of the wake was confirmed by running different tests with the probe blocked at different positions in this wake, i.e., without being influenced by the frequency response of the system. The loss coefficient was defined as follows:

$$\zeta_2 = 1 - \frac{V_2^2}{V_{2,is}^2}$$

$$\zeta_2 = 1 - \frac{1 - \left(\frac{p_2}{p_{02}}\right)^{\frac{k-1}{k}}}{1 - \left(\frac{p_2}{p_{01}}\right)^{\frac{k-1}{k}}}$$

The downstream integrated loss coefficient distribution of Fig. 16 was finally obtained as a function of the isentropic exit Mach number. The uncertainty on this loss coefficient was estimated to be 0.2 points. No significative effects of downstream Reynolds number were observed. The general level of the losses, measured for 1 percent free-stream turbulence, is quite low. This is explained by the late transition observed for all Mach and Reynolds number configurations at low turbulence intensity during the heat transfer measurements. Some more confidence in these results was found when comparing them with a classical boundary layer calculation performed by Happel and Ramm (1989) at MTU, Germany for $M_{2,is}=1.0$. This boundary layer program, based on an integral method, predicts boundary layer losses of the order of 1 percent. To this number one should add trailing edge losses, evaluated at 0.75 percent, base pressure losses, almost zero in this particular situation and shock losses, estimated at 0.5 percent. This reasonable overall estimation is consistent with the measured value.

Because of the lack of a detailed angular calibration of the probe at different Mach numbers, only one result will be presented here (Fig. 16) and compared with the calculated values obtained from the two dimensional inviscid predictions. The uncertainty associated with this angle measurement is most probably of the order of ± 0.5 deg. More detailed work on this subject is presently under way.

Summary—Conclusion

Detailed aerodynamic and convective heat transfer measurements have been obtained on a high-pressure turbine nozzle guide vane, looking at the effect of free-stream Mach and Reynolds numbers as well as turbulence intensity. The measurements were taken using the VKI short duration compression tube facility and were compared to some extent to the results obtained from in-house available two-dimensional inviscid and boundary layer programs.

The aim of this investigation is to provide detailed information about the flow field in this cascade for operating conditions similar to those observed in real engines in order to allow the evaluation of both advanced inviscid and viscous turbomachinery calculation methods. A complete, tabulated description of the aerodynamic and heat transfer experimental results is available from the authors upon request.

References

Arts, T., 1982, "Cascade Flow Calculations Using a Finite Volume Method," in: *Numerical Methods for Flows in Turbomachinery Bladings*, V.K.I. Lecture Series 1982-07.

Arts, T., Lambert de Rouvroit, M., and Sieverding, C. H., 1989, "Contribution to the Workshop on Two Dimensional Inviscid and Viscous Turbomachinery Flow Calculations," in: *Numerical Methods for Flows in Turbomachinery*, V.K.I. Lecture Series 1989-06.

Consigny, H., and Richards, B. E., 1982, "Short Duration Measurements of Heat Transfer Rate to a Gas Turbine Rotor Blade," ASME *Journal of Engineering for Power*, Vol. 104, No. 3, pp. 542-551.

Crawford, M. E., 1986, "Simulation Codes for Calculation of Heat Transfer to Convectively-Cooled Turbine Blades," in: *Convective Heat Transfer and Film Cooling in Turbomachinery*, V.K.I. Lecture Series 1986-06.

Crawford, M. E., 1988, Private Communication.

Happel, H. W., and Ramm, G., 1989, "Contribution to the Workshop on Two Dimensional Inviscid and Viscous Turbomachinery Flow Calculations," in *Numerical Methods for Flows in Turbomachinery*, V.K.I. Lecture Series 1989-06.

Jones, T. V., Schultz, D. L., and Hendley, A. D., 1973, "On the Flow in an Isentropic Free Piston Tunnel," ARC R&M 3731.

Patankar, S. V., and Spalding, D. B., 1967, *Heat and Mass Transfer in Boundary Layers*, 1st ed., Morgan-Grampian, London.

Richards, B. E., 1980, "Heat Transfer Measurements Related to Hot Turbine Components in the von Karman Institute Hot Cascade Tunnel," in: *Testing and Measurement Techniques in Heat Transfer and Combustion*, AGARD CP 281, Paper 6.

Schlichting, H., 1968, *Boundary Layer Theory*, 6th ed., McGraw-Hill, New York.

Schultz, D. L., and Jones, T. V., 1973, Heat Transfer Measurements in Short Duration Hypersonic Facilities," AGARDograph 165.

Schultz, D. L., Jones, T. V., Oldfield, M. L. G., and Daniels, L. C., 1978, "A New Transient Facility for the Measurement of Heat Transfer Rates," in: *High Temperature Problems in Gas Turbine Engines*, AGARD CP 229.

Sieverding, C. H., 1973, "Sample Calculations—Turbine Tests," in: *Transonic Flows in Turbomachinery*, V. K. I. Lecture Series 59.

Sieverding, C. H., 1982, "Workshop on Two Dimensional and Three Dimensional Flow Calculations in Turbine Bladings," in: *Numerical Methods for Flows in Turbomachinery Bladings*, V. K. I. Lecture Series 1982-07.

Sieverding, C. H., Arts, T., Pasteels, M.-H., and Klinger, P., 1988, "Transonic Cascade Performance Measurements Using a High Speed Probe Traversing Mechanism in a Short Duration Wind Tunnel," presented at the 9th Symposium on Measuring Techniques for Transonic and Supersonic Flow in Cascades and Turbomachines, Oxford, United Kingdom.

Smith, M. C., and Kuethe, A. M., 1966, "Effects of Turbulence on Laminar Skin Friction and Heat Transfers," *Physics of Fluids*, Vol. 9, No. 12, p. 2337.

Van den Braembussche, R. A., Leonard, O., and Nekmouche, L., 1989, "Subsonic and Transonic Blade Design by Means of Analysis Codes," presented at the 64th FDP specialists' meeting on "Computational Methods for Aerodynamic Design (Inverse) and Optimization," Loen, Norway.